EEET ECOLOGICAL ENGINEERING & ENVIRONMENTAL TECHNOLOGY

Ecological Engineering & Environmental Technology, 2025, 26(5), 349–365
https://doi.org/10.12912/27197050/203461
ISSN 2719–7050, License CC-BY 4.0

Received: 2025.03.03
Accepted: 2025.03.25
Published: 2025.04.01

Normalised difference vegetation index-based vegetation dynamics analysis to identify differences in climate variability during La Nina and El Nino phases in Gowa Regency

Ari Affandy Mahyuddin[1*], Samsu Arif[2], Darhamsyah[3]

[1] Environmental Management Study Program, Graduate School, Hasanuddin University, Makassar 90245, Indonesia
[2] Department of Geophysics, Faculty of Mathematics and Natural Sciences, Hasanuddin University, Makassar 90245, Indonesia
[3] Environmental Management Study Program, Graduate School, Hasanuddin University, Makassar 90245, Indonesia
* Corresponding author's e-mail: ariaffandymahyuddin@gmail.com

ABSTRACT

A deeper understanding of the influence of the El Nino-southern oscillation (ENSO) on climate variability in a region is essential to anticipate its future impacts.Vegetation dynamics can be an indicator of climate variability due to its sensitivity to environmental changes. Therefore, this study aims to analyse vegetation dynamics based on normalised difference vegetation index (NDVI) to identify differences in climate variability in the La Nina and El Nino phases in Gowa Regency, and to analyse the relationship between climate parameters and vegetation dynamics. The La Nina phase observed was in July-September in 2022, while the El Nino phase was in the same months in 2023 to provide more accurate comparison results, both phases were confirmed based on the multivariate ENSO index (MEI). Remote sensing data from Sentinel-2 L2A satellite images were analysed using ArcGIS 10.8 software with the NDVI method. Furthermore, spatial and temporal analyses were conducted to compare vegetation dynamics in both phases. The results showed a significant difference in vegetation dynamics between La Nina and El Nino phases. During the La Nina phase in 2022, NDVI showed stability and dominance of areas with high vegetation indices. Climate variability in this phase is characterised by stable rainfall and air temperature, which support optimal vegetation growth. In contrast, during the El Nino phase in 2023, NDVI shows a significant decrease in areas with a high vegetation index and a significant increase in areas without vegetation. Climate variability during this phase is characterised by very low rainfall and higher air temperatures, which has implications for reduced productivity and vegetation degradation. In addition, regression analyses showed that air temperature tends to have a greater influence than rainfall on vegetation dynamics. The regression model has an $R^2 = 0.92$ and Adjusted $R^2 = 0.87$, indicating strong predictive ability. Partially, the two variables showed no significant influence at the 95% confidence level. However, based on F statistics ($F = 17.63$; $p = 0.02$), both variables simultaneously had a significant influence on vegetation. This research can be used as a basis for formulating mitigation and adaptation strategies to climate variability in the future.

Keywords: NDVI, ENSO, La Nina, El Nino, vegetation, gowa regency.

INTRODUCTION

In Indonesia, climate variability can be influenced by the El Nino and La Nina phenomena, collectively referred to as the El Nino-southern oscillation (ENSO) (Nur'utami & Hidayat, 2016). El Nino is characterised by an increase in the equatorial temperatures of the central and eastern Pacific, while La Nina is characterised by a cooling of sea surface temperatures in the same region (Damette et al., 2024). The impact of these two phenomena is globally widespread and affects rainfall patterns and air temperatures in countries around the world (Santoso et al., 2017). ENSO has been widely recognised as a major factor in the unpredictability of seasonal patterns, as it can cause extreme rainfall during La Nina and prolonged drought during El Nino (Arjasakusuma et al., 2018; Kurniadi et al., 2021). Uncertainty in seasonal patterns due to ENSO can disrupt ecosystem stability (Wang et al., 2020).

The Meteorology, Climatology and Geophysics Agency reports that from July to September 2022, under the influence of La Nina, rainfall in Indonesia will be higher than the 30-year long-term average, with an earlier start of the rainy season, especially in Java, Sulawesi, Kalimantan, Maluku, Papua and southern Sumatra (BMKG, 2022). The following year, from July to September in 2023 under the influence of El Nino, Indonesia experienced drier than normal conditions, with rainfall falling 30% below normal, especially in Java, Bali, Nusa Tenggara, and Sulawesi (BMKG, 2023). Based on this, Gowa Regency, which is located in South Sulawesi, is certainly inseparable from these two ENSO phases which can affect climate variability in this region. Along with the increasing frequency and intensity of the ENSO phenomenon due to global climate change (Mishra et al., 2022). A deeper understanding of how La Nina and El Nino affect climate variability differently in a region, especially at the local level, is crucial to anticipate their future impacts

One aspect that can reflect the influence of ENSO on climate variability is the response given by the ecosystem. One component of the ecosystem that has a high sensitivity to climate variability is vegetation (Bao et al., 2021). In addition, information on how vegetation growth is affected by climate variability is still needed (Le, 2023), because it has not been discussed comprehensively, especially based on spatial and temporal distribution (Sun et al., 2022). Remote sensing technology enables spatial and temporal analyses that cannot be done with conventional methods, providing accurate data on vegetation variability (Xu et al., 2024). The normalised difference vegetation index (NDVI) method is one approach in remote sensing that is widely used to monitor vegetation dynamics (Li et al., 2024). NDVI is very useful in understanding vegetation dynamics, such as monitoring plant health and productivity spatially and temporally (Zhihao & Fang, 2024). Therefore, NDVI analysis can be used to observe how vegetation dynamics respond to climate variability during La Nina and El Nino phases in Gowa Regency Several previous studies have looked at how ENSO affects climate variability in different regions (Zhu et al., 2021; Sarvina, 2023; Stuecker, 2023). However, there are still limitations in understanding how ENSO, especially in the La Nina phase in 2022 and El Nino in 2023, affects climate variability differently at the local level such as Gowa Regency, by looking at vegetation dynamics through NDVI. This is supported by Wiel & Bintanja (2021) in his research concluded that in many regions, climate variability is still not well understood in a comprehensive manner. Therefore, this research can contribute to the gap. Understanding how ENSO affects climate variability at the local level is important because it can affect rainfall patterns and air temperature, which can have implications for ecosystem instability. Therefore, this study aims to analyse NDVI-based vegetation dynamics that can be an indicator of differences in climate variability during La Nina and El Nino phases in Gowa Regency. The results of this study are expected to provide empirical evidence of how the influence of ENSO, especially La Nina and El Nino, affects climate variability in Gowa Regency differently, so that it can be used as a basis for formulating mitigation and adaptation strategies in the future.

MATERIAL AND METHODS

Research area

Gowa Regency is one of the Indonesian regions affected by the ENSO climate phenomenon, namely La Nina in 2022 and El Nino in 2023 based on information released by BMKG. As shown in Figure 1. as part of Gowa Regency, Manuju and Parangloe sub-districts which are the focus areas of the research are located at the coordinates of 5°20’45” LS, 119°43’06” BT dan 5°18’12” LS, 119°47’48” BT. Gowa Regency consists of 18 subdistricts. However, this research has limitations in the scope of the study area that need to be considered. This research only covers two subdistricts, namely Manuju and Parangloe. This is based on two main reasons. Firstly, the Sentinel-2A satellite imagery used for this study, during the La Nina phase in 2022 (July-September) and the El Nino phase in 2023 (July-September), showed that most sub-districts in Gowa Regency were cloud-covered, making it impossible to accurately and consistently conduct spatial and temporal analyses of NDVI across all subdistricts. Secondly, most of the other sub-districts are dominated by two types of land cover, namely settlements and agricultural land, which limits the overall analysis of vegetation dynamics.

Manuju and Parangloe sub-districts were chosen because during the observation period, they were not covered by clouds as seen in the satellite images analysed. In addition, these two areas are dominated by various types of vegetation, so that

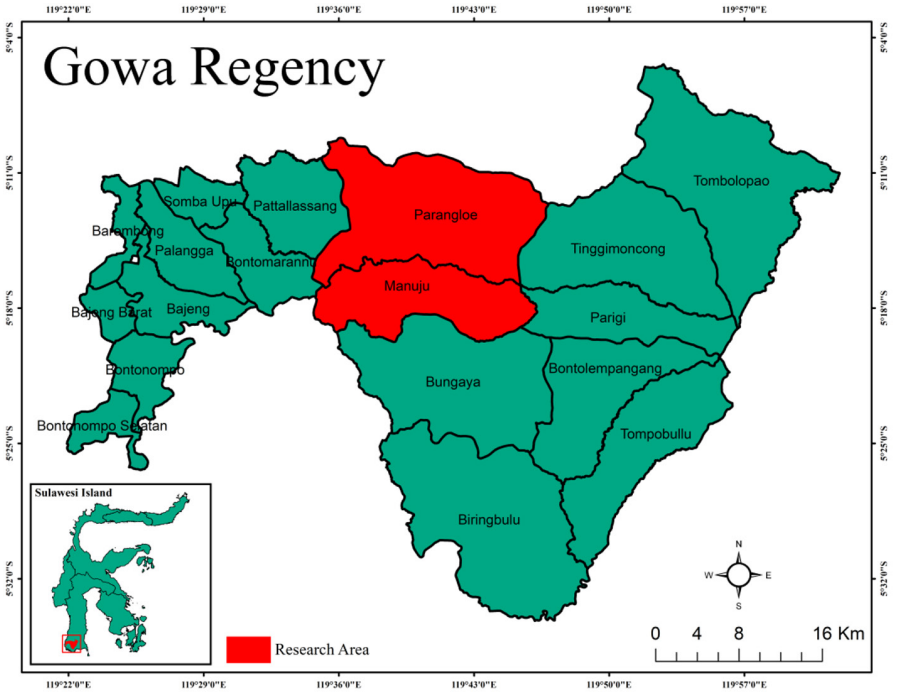

Figure 1. Research area Manuju and Parangloe sub-districts Gowa Regency

the analysis carried out is more in line with the research objectives. The various types of vegetation that dominate in the two sub-districts include forests, shrubs and grasses, and agricultural land. This makes the two sub-districts a representative model for understanding patterns of vegetation dynamics that are relevant to the ecosystem as a whole in Gowa Regency. Although this study was limited to two sub-districts, the results obtained are still relevant to understanding vegetation dynamics as an indicator of differences in climate variability in Gowa Regency during the La Nina and El Nino phases.

Data source

Satellite imagery

The metadata information of the downloaded satellite images can be seen in Table 1. This table contains information about all the images analysed in this study. Based on the results of research conducted by Sandera & Stych (2020) found that Sentinel-2 satellite imagery has the best resolution, both spatially and temporally in monitoring changes in various types of vegetation. The higher resolution of a satellite image will provide more detailed analysis results (Galar et al., 2019).

Table 1. Sentinel-2 L2A characteristic features of satellite data

Name	Level	Date	Band	Resolution
T50MQV_20220728T022341_B04	2A	28/07/2022	4 (Red)	10 meters
T50MQV_20220822T022341_B04	2A	22/08/2022	4 (Red)	10 meters
T50MQV_20220911T022341_B04	2A	11/09/2022	4 (Red)	10 meters
T50MQV_20230728T022331_B04	2A	28/07/2023	4 (Red)	10 meters
T50MQV_20230827T022331_B04	2A	27/08/2023	4 (Red)	10 meters
T50MQV_20230911T022331_B04	2A	26/09/2023	4 (Red)	10 meters
T50MQV_20220728T022341_B08	2A	28/07/2022	8 (NIR)	10 meters
T50MQV_20220822T022341_B08	2A	22/08/2022	8 (NIR)	10 meters
T50MQV_20220911T022341_B08	2A	11/09/2022	8 (NIR)	10 meters
T50MQV_20230728T022331_B08	2A	28/07/2023	8 (NIR)	10 meters
T50MQV_20230827T022331_B08	2A	27/08/2023	8 (NIR)	10 meters
T50MQV_20230926T022331_B08	2A	26/09/2023	8 (NIR)	10 meters

Vegetation type land cover

Land cover vegetation type data used in this study was obtained from Esri Land Cover. ESRI land cover provides remote sensing-based data with global resolution that is updated annually. This data is used as a reference which is then corrected to map land cover conditions in the research area, namely Manuju District and Parangloe District, Gowa Regency. In this study, there are three types of vegetation observed, namely tree vegetation, shrub and rumuput vegetation and agricultural land vegetation to see their respective responses to climate variability.

ENSO conditions (La Nina phase in 2022 and El Nino phase in 2023)

Multivariate ENSO index (MEI) is used to provide information related to ENSO events, especially La Nina and El Nino, which can affect climate variability. Based on Figure 2, it can be seen that in 2022 in July-September there were La Nina conditions, while in 2023 in July-September there were El Nino conditions. The value for each month is obtained directly from the data provided by NOAA without going through any calculation process.

The MEI is a method used to measure the intensity of the ENSO. The MEI is considered the most comprehensive index for monitoring ENSO as it incorporates the analysis of six different meteorological parameters measured in the tropical Pacific (Mazzarella et al., 2010).

Climate parameters

In this study, two climate parameters are used as a reference because they are related to ENSO conditions, namely rainfall and air temperature (Chueasa et al., 2024; Kemarau & Eboy, 2021). The average rainfall and air temperature can be seen in Table 2. The climate parameter data used in this study were obtained from the Meteorology, Climatology and Geophysics Agency (BMKG) through an official request mechanism in accordance with applicable institutional procedures. This data is not available for public access through the BMKG website due to regulations regarding the distribution of official data to ensure validity and governance in accordance with national policies. Requests for data are made through academic institutions by completing an official form, a letter of request explaining the purpose of using the data, and approval from relevant parties at BMKG. This process aims to ensure the transparency, accuracy and credibility of the data used in this study.

These two parameters serve as key indicators of climate variability. The information on both graphs is used to describe the climate variability in July-September 2022 during the La Nina phase and the same months in 2023 during the El Nino phase. Data on these two parameters provide a snapshot of how ENSO-driven climate variability materialises in the research area (Fig. 3 and 4).

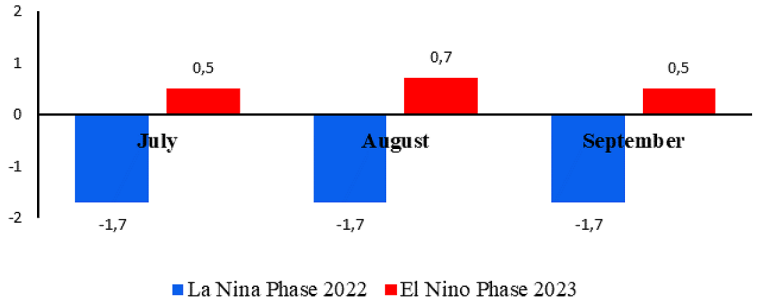

Figure 2. Graph value the multivariate ENSO index. National Oceanic and Atmospheric Administration (NOAA) (https://psl.noaa.gov/enso/mei/#data)

Table 2. Climate parameters

Climate parameters	La Nina phase 2022			El Nino phase 2023		
	July	August	September	July	August	September
Average rainfall (mm)	59	63	59	94	0	0
Average air temperature (°C)	26.9	26.9	27.2	26.8	27.1	28.3

Note: Meteorology, climatology and geophysics agency (BMKG)

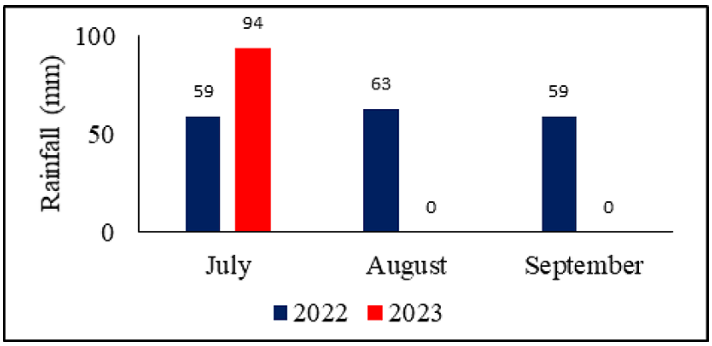

Figure 3. Average rainfall chart

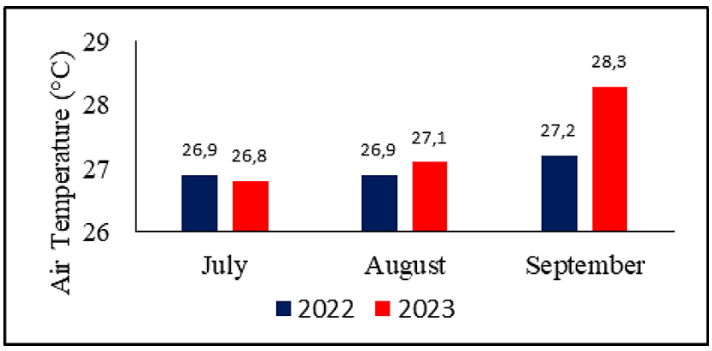

Figure 4. Average air temperature chart

Processing

In this research, the NDVI analysis was conducted using ArcGIS 10.8 software by utilising Sentinel-2 satellite imagery. The processing stage begins with the collection of Sentinel-2 imagery from official data sources in accordance with the observed period. Next, pre-processing was performed, such as cropping the area according to the boundaries of the study area. After that, the reflectance values of the relevant spectral channels were extracted to produce NDVI maps. This process was carried out in ArcGIS 10.8 using the Raster Calculator feature to process the pixel values of the corrected image. The results of the calculation were then visualised in the form of thematic maps showing the variation of NDVI values. After that, an analysis was carried out to see the changes in area based on the NDVI classification during the observed period.

NDVI calculation

NDVI is the most commonly used vegetation index to describe the greenness of vegetation as it is sensitive to chlorophyll abundance and photosynthetically active leaves (Martinez & Labib, 2023). The NDVI formula is calculated using the following formula:

$$\text{NDVI} = \frac{NIR-RED}{NIR+RED} \quad (1)$$

where: NIR represents the Nir Infrared band and RED represents the Red band (Mehmood et al., 2024). On Sentinel-2A, it is calculated with the following formula:

$$\text{NDVI} = \frac{Band\ 8-Band\ 4}{Band\ 8+Band\ 4} \quad (2)$$

NDVI classification

In NDVI analysis, the vegetation index density can be seen from a range of values -1 to +1, which in general larger index values indicate better health and density than smaller values, and can be used as primary data because it has a positive correlation with field conditions (Akbar et al., 2020). The NDVI value classification range can be seen in Table 3.

The NDVI classification in this study was adjusted based on the analysis of Sentinel-2 imagery in the study area. The steps taken were:

a) Review of NDVI classification, previous studies (Amanollahi et al., 2012; Atun et al., 2020; Aquino et al., 2018; Aziz et al., 2018; Bid, 2016) compared to see how the NDVI classification boundaries differed.
b) NDVI value extraction, NDVI values were

Table 3. NDVI value classification range

Class	Classification	NDVI range
1	Water body	NDVI ≤ 0
2	No vegetation	0 < NDVI ≤ 0.2
3	Low vegetation index	0.2 < NDVI ≤ 0.3
4	Moderate vegetation index	0.3 < NDVI ≤ 0.5
5	High vegetation index	0.5 < NDVI ≤ 1

collected from reference sites using supervised classification in ArcGIS 10.8.

c) Cut-off values adjustment, the distribution of NDVI values was analysed to determine classification limits that better suit the conditions of the study area.

d) The final classification, based on the analysis, established five main categories: water body (NDVI ≤ 0); No vegetation (0 < NDVI ≤ 0.2); Low vegetation index (0.2 < NDVI ≤ 0.3); Medium vegetation index (0.3 < NDVI ≤ 0.5); High vegetation index (0.5 < NDVI ≤ 1). This adjustment ensures that the NDVI classification used more accurately represents the vegetation condition in the study area.

Data analysis technique

Multicollinearity test

This study conducted a multicollinearity test whose function is to identify linear relationships between independent variables (Shrestha, 2020). This test is carried out by looking at the variance inflation factor (VIF) value, with the VIF value criterion <5 (Akinwande et al., 2015). Multicollinearitytestwas performed by calculating the variance inflation factor (VIF) for the rainfall (X_1) and air temperature (X_2) variables. VIF is calculated based on the coefficient of determination (R^2) of regression between independent variables, with the model:

$$\text{Regression 1: } X_1 = \beta_0 + \beta_1 X_2 + \varepsilon$$

$$\text{Regression 2: } X_2 = \beta_0 + \beta_1 X_1 + \varepsilon \quad (3)$$

where: X_1 – rainfall, X_2 – air temperature, β_0 – the intercept, β_1 – regression coefficient, ε – error term

After obtaining R^2 from each regression, the VIF value is calculated using the formula:

$$VIF_i = \frac{1}{1 - R_i^2} \quad (4)$$

where: VIF_i – variance inflation factor for variable I, R_i^2 – coefficient of determination from regression of variable i on other variables

The average values of rainfall and air temperature for each month are presented in Table 4.

Multiple linear regression analysis

A regression model that involves one dependent variable and more than one independent variable is called multiple linear regression (Uyanık & Guler, 2013). This analysis makes it possible to measure the extent to which each independent variable (rainfall and air temperature) affects the dependent variable (vegetation area at NDVI). The multiple linear regression model in this study is as follows:

$$\hat{Y} = \beta_0 + \beta_1 X_1 + \beta_2 X_2 \quad (5)$$

where: $\hat{Y}$ – vegetation area, β_0 – the intercept of the line on the $\hat{Y}$ axis, β_1, β_2 – coefficient of multiple lines regression, X_1 – rainfall, X_2 – air temperature

Table 4. Average rainfall and air temperature values

Years	Month	Rainfall (mm)	Air temperature (°C)
2022	July	59	26.9
2022	August	63	26.9
2022	September	59	27.2
2023	July	94	26.8
2023	August	0	27.1
2023	September	0	28.3

Furthermore, calculations of R^2, Adjusted R^2, and F-Statistics were used to evaluate the quality of the multiple linear regression model in explaining the relationship between rainfall and air temperature on vegetation. The coefficient of determination (R^2) indicates the extent to which rainfall and air temperature can explain variations in vegetation. The R^2 value is calculated using the following formula:

$$R^2 = 1 - \frac{SS_{res}}{SS_{total}} \quad (6)$$

where: SS_{res} – sum of squares residual, SS_{total} – sum of squares total

R^2 values range from 0 to 1, where values close to 1 indicate that the regression model is very good at explaining variations in the data. Because the number of independent variables in the model can affect the R^2 value, Adjusted R^2 is used to adjust for the influence of the number of variables. The calculation is:

$$R^2{}_{adj} = 1 - \left(\frac{(1 - R^2)(n-1)}{n - k - 1}\right) \quad (7)$$

where: n – number of observations (amount of data), k – number of independent variables in the model.

Adjusted R^2 is more accurate in evaluating regression models, especially if the number of independent variables increases. To assess the significance of the overall model, the F-Statistic test is used, which is calculated by the formula:

$$F = \frac{\text{MSR}}{\text{MSE}} = \frac{(SS_{reg}/k)}{(SS_{res}/(n - k\ 1))} \quad (8)$$

where: SS_{reg} – sum of squares regression, SS_{res} – sum of squares residual, MSR – mean square regression, MSE – mean square error, n – jumlah observasi, k – jumlah variabel independen.

F statistics to determine whether the independent variables in simultas (overall) are significant to the dependent variable (Sureiman & Mangera, 2020). In this test Fhitung (Sig) is compared with Ftabel at the 95% confidence level or $\alpha = 5\%$ with the following conditions if sig < 0.05 then H0 is rejected (real). If sig > 0.5 then H0 is accepted (not real).

RESULTS AND DISCUSSION

NDVI-based vegetation dynamics as an indicator of differences in climate variability during La Nina and El Nino in Gowa district

Based on the results of the NDVI analysis that has been carried out, it can be seen in Figures 5, 6, and 7 are maps that show the dynamics of vegetation in the La Nina period in 2022 in July-September, while Figures 8, 9, and 10 show the dynamics of vegetation in the El Nino period in 2023 in the same month. This analysis was conducted to identify differences in the spatial pattern of NDVI, which is divided into 5 classifications. Each classification is represented with a different colour as shown on the map, so that visually there can be clearly observed differences in vegetation dynamics based on NDVI between the La Nina

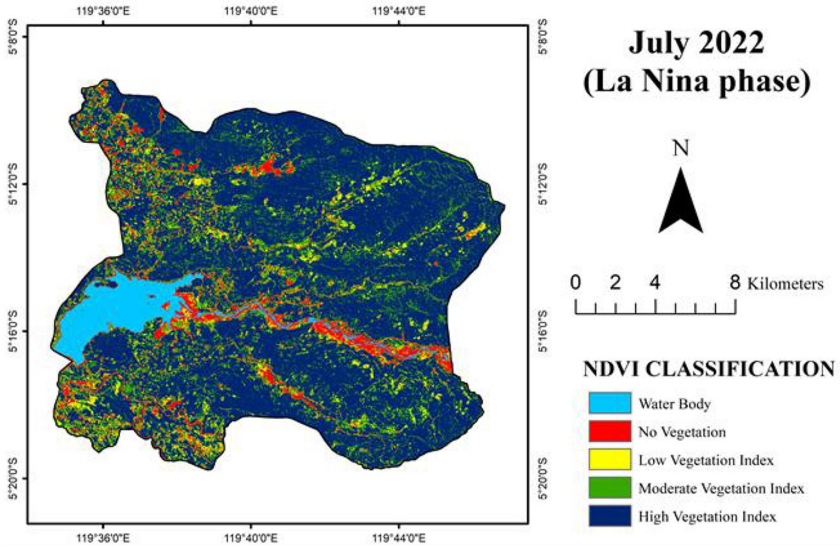

Figure 5. NDVI in July 2022 during La Nina phase

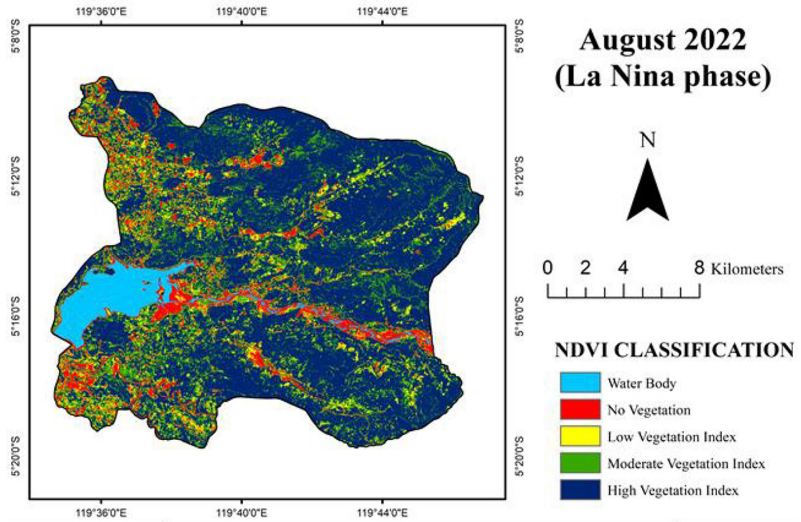

Figure 6. NDVI in August 2022 during La Nina phase

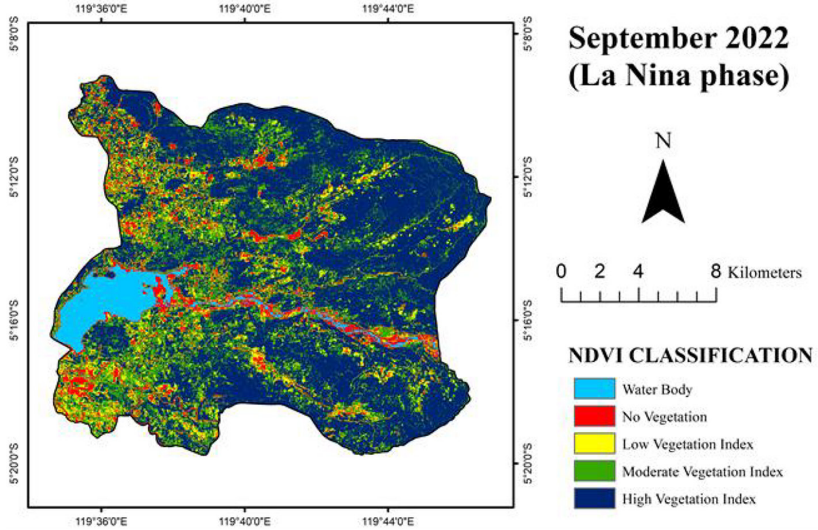

Figure 7. NDVI in September 2022 during La Nina phase

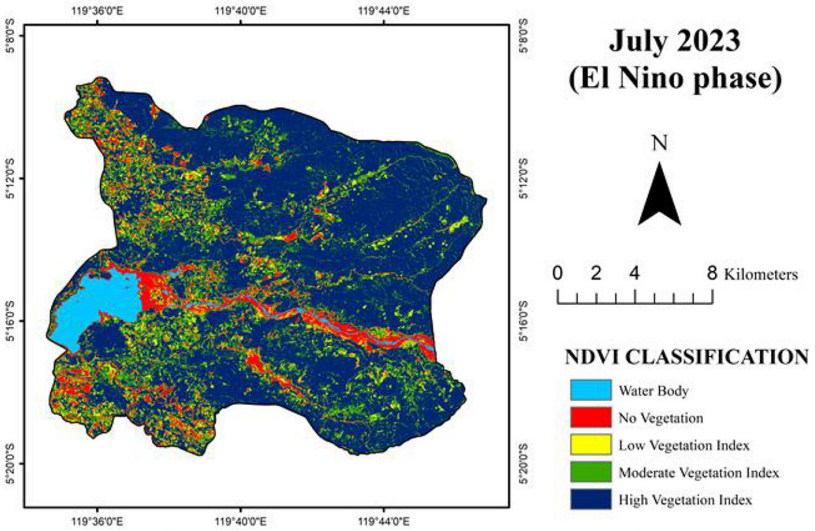

Figure 8. NDVI in July 2023 during El Nino phase

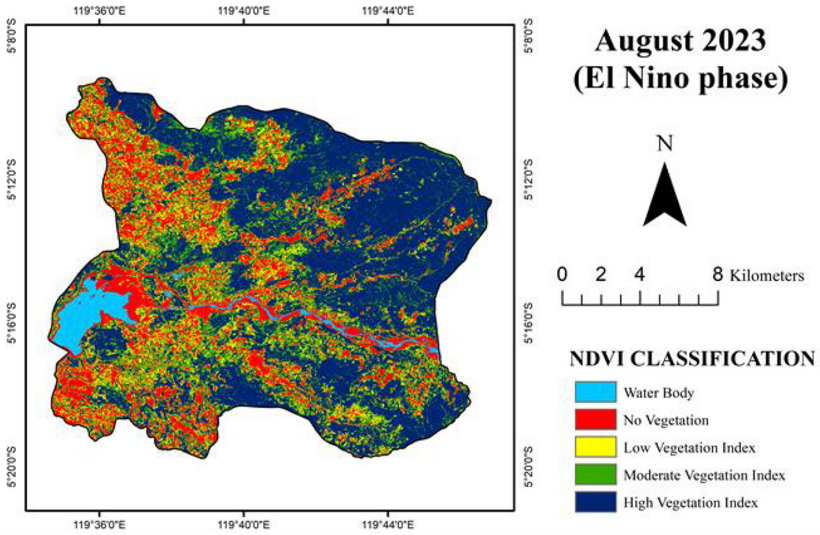

Figure 9. NDVI in August 2023 during El Nino phase

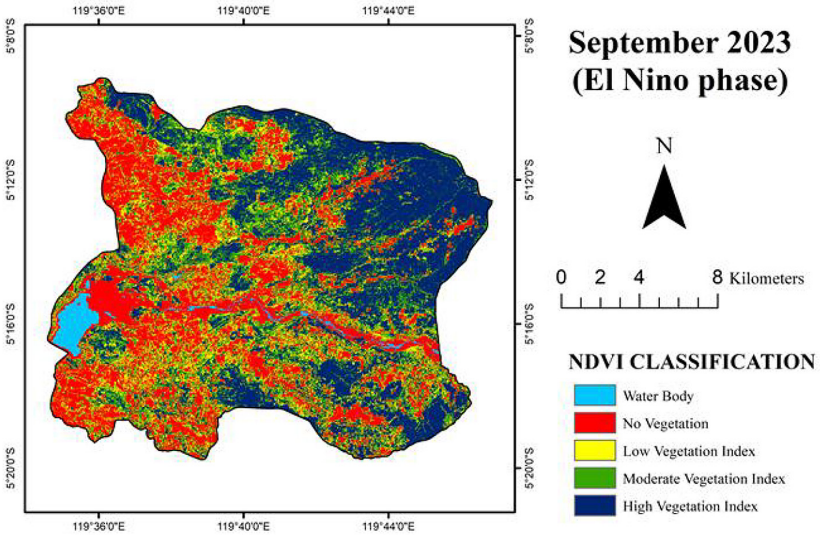

Figure 10. NDVI in September 2023 during El Nino phase

phase in 2022 and the El Nino phase in 2023, which can provide an initial picture of the differences in climate variability in the two phases.

The results of the NDVI map analysis were further analysed in ArcGis 10.8 software to quantitatively determine the extent of each of the five NDVI classifications in each period. Table 5 shows the results of the analyses that have been carried out as well as the visualisation can be seen in Figure 5 to Figure 10 which provides an overview of vegetation dynamics. To facilitate interpretation of the changing trends, the results of this analysis are also visualised in graphical form in Figure 11.

The vegetation dynamics described from the analysis results are interpreted based on ENSO conditions, especially the La Nina phase in 2022 and EL Nino in 2023 confirmed through the MEI in Figure 2, as well as climate variability based on two climatic parameters, namely rainfall and air temperature whose data are obtained from BMKG. Indonesia has a recurring annual seasonal pattern cycle, namely the rainy and dry seasons, meaning that the same month in different years has the same climate variability. Climate parameters, especially rainfall and air temperature in Table 3 show that climate variability in the La Nina phase in 2022 is different from climate variability in the El Nino phase in 2023, even though the months compared are the same, namely July, August and September. The results of spatial and

Table 5. Change rate of vegetation area based on NDVI classification

NDVI Classification	La Nina 2022 (ha)			El Nino 2023 (ha)		
	July	August	September	July	August	September
Water body	1.592	1.488	1.437	1.197	921	546
No vegetation	1.795	2.301	2.176	2.337	5.643	9.170
Low vegetation index	1.788	2.195	2.523	2.043	3.671	4.422
Moderate vegetation index	5.404	6.262	7.252	5.392	6.182	6.738
High vegetation index	20.539	18.873	17.729	20.150	14.701	10.244

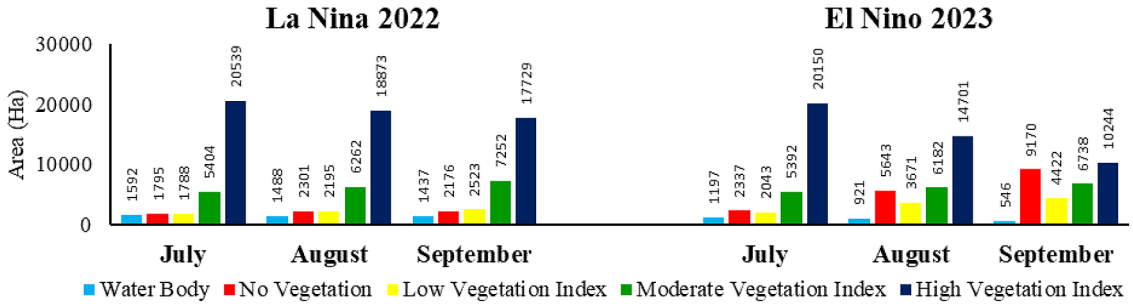

Figure 11. Distribution of vegetation area based on NDVI

temporal analyses of vegetation dynamics based on NDVI can provide empirical evidence of this.

Climate variability during the La Nina phase in 2022 in July, August, and September, can be seen in Table 3, which shows that the average rainfall was 59 mm, 63 mm, and 59 mm, while the average air temperature was 26.9°, 26.9°, and 27.2°. Based on Figures 5, 6, and 7, which show the spatial and temporal dynamics of vegetation in this period, stable rainfall and air temperature are able to support vegetation productivity, as evidenced by the dominance of areas with high and medium vegetation indices. However, areas with low vegetation index and no vegetation slightly increased from July to September, possibly due to the seasonal transition from the rainy season to the dry season in accordance with Indonesian seasonal patterns. In addition, the pattern of the community's planting season, which is closely related to the growth phase of plants on agricultural land, is also the cause. In their research Adinda et al. (2020) stated that the phase of plant growth on agricultural land can affect the results of NDVI analysis.

In contrast, the climatic variability in the El Nino phase of 2023 in the same month can also be seen in Table 3, which shows that the average rainfall was 94 mm, 0 mm, and 0 mm, respectively, while the average air temperature was 26.8°, 27.1°, and 28.3°, respectively. Based on Figures 8, 9, and 10, which show the spatial and temporal vegetation dynamics of the period, the very low rainfall and high air temperature, especially in August-September, caused a significant decrease in areas with a high vegetation index, as well as an increase in areas with a low vegetation index and areas without vegetation, indicating vegetation degradation. This shows the sensitivity of vegetation to extreme climate variability during the El Nino phase, where vegetation that depends on water availability and stable air temperature becomes vulnerable to rapid changes in environmental conditions. This is because significant soil moisture loss can inhibit photosynthesis (Didion-Gency et al., 2022).

ENSO dynamics on climate variability also have an impact on the water body of the Bili-Bili reservoir in the study area. During the La Nina phase, the water body area of Bili-Bili reservoir appeared to be stable, while during the El Nino phase, the water body area decreased drastically by about 59% from July to September due to increased evaporation and lack of rainfall which also confirmed the strong relationship between ENSO and water availability. Overall, the findings confirm that the ENSO phenomenon, which includes La Nina and El Nino, contributes to climate variability specifically in Gowa Regency, which is reflected by the vegetation dynamics based on NDVI.

Using a remote sensing-based NDVI approach, this study identifies spatial and temporal patterns of changes in vegetation dynamics that are closely related to climate variability in the form of rainfall variability and air temperature influenced by ENSO. The findings emphasise the importance of understanding how ENSO contributes to local climate variability. Such insights can contribute to mitigation and adaptation efforts against the negative impacts of ENSO-related extreme weather events, thereby strengthening community resilience as well as the local economy.

Although during the El Nino phase there was a large negative impact on vegetation, it should be noted that some areas were still able to survive with healthy vegetation. Diverse vegetation types will respond differently to climate variability (Li et al., 2024). Areas with vegetation that is more resistant to dry conditions may show better resilience to stresses caused by El NinoIn this study, three types of vegetation, namely tree vegetation, shrub and grass vegetation, and agricultural land, were also analysed to observe their respective responses to climate variability influenced by ENSO. The results of the previous spatial and temporal analyses of NDVI were combined with land cover information from Esri Land Cover through a clipping process to extract the NDVI values of each vegetation type.

Tree vegetation

Table 6 shows the quantitative changes in tree vegetation area. The change in area in hectares (ha) based on 5 NDVI classifications shows the difference and change in area in each classification during the La Nina phase in 2022 and the El Nino phase in 2023. To clarify the pattern of changes in tree vegetation during the study period, the results of the analysis are visualised in the form of a graph in Figure 12 to facilitate the interpretation of the trend of changes that occur.

Tree vegetation showed stability with a relatively large area of high vegetation index in each month during the La Nina phase in 2022. In contrast, during the El Nino phase in 2023, the area of high vegetation index decreased, while the area of low vegetation index increased, especially in September, indicating vegetation stress due to dry conditions. Lack of water supply can cause disturbances in the process of water absorption through the roots, which has a direct impact on reducing photosynthetic efficiency (Nugroho & Setiawan, 2022). This is consistent with the results of the NDVI analysis, because in addition to the density level, NDVI is also highly dependent on the photosynthesis process of plants. However, the results of this study show that the decline in productivity in tree vegetation is not too significant, indicating that tree vegetation has good resilience to dry climate variability during the El

Table 6. Rate of change of tree vegetation area based on NDVI classification

NDVI classification	La Nina 2022 (ha)			El Nino 2023 (ha)		
	July	August	September	July	August	September
Water body	0	0	0	0	0	0
No vegetation	0	0	0	0	0	0
Low vegetation index	306	340	336	304	912	2249
Moderate vegetation index	2526	2906	3342	2002	3846	5669
High vegetation index	15911	15486	15071	16433	13715	9900

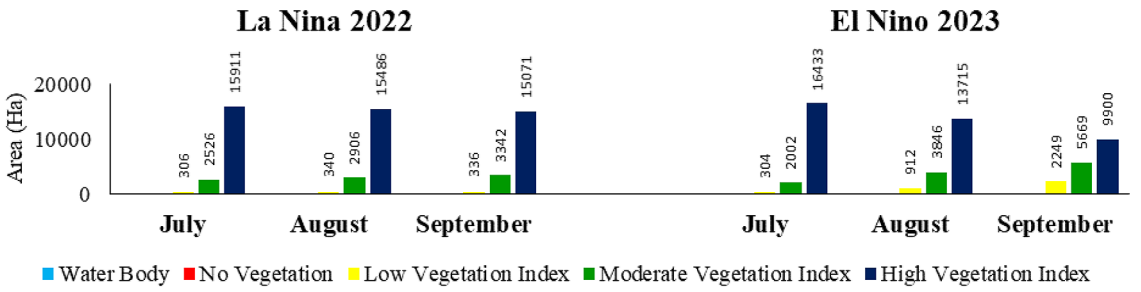

Figure 12. Distribution of tree vegetation area based on NDVI

Nino phase in 2023, but can still be degraded under more extreme drought conditions.

Shrub and grass vegetation

Table 7 shows quantitative changes in the area of shrub and grass vegetation. The change in area in hectares (ha) based on 5 NDVI classifications shows the difference and change in area for each classification during the La Nina phase in 2022 and the El Nino phase in 2023. To clarify the pattern of changes in shrub and grass vegetation during the study period, the results of the analysis are visualised in graphical form in Figure 13 to facilitate interpretation of the changing trends.

Shrub and grass vegetation showed a faster response to changes in climate variability. During the La Nina phase in 2022, areas with a high vegetation index dominated, but during the El Nino phase in 2023, there was a drastic decrease especially in September, with areas of high vegetation shrinking significantly and unvegetated areas increasing and dominating. Shrubs and grasses typically interact competitively (Letts et al., 2010). Physiologically, shrubs have higher resistance to drought compared to the more sensitive grasses (Winkler et al., 2019). This indicates that the shrinkage of high and medium vegetation index areas, and the increase of low and unvegetated vegetation index areas, were dominated by grass vegetation.

Farmland vegetation

Table 8 shows the quantitative changes in agricultural land vegetation area. The change in area in hectares (ha) based on 5 NDVI classifications shows the difference and change in area in each classification during the La Nina phase in 2022 and the El Nino phase in 2023. To clarify the pattern of changes in agricultural land vegetation during the study period. The results of the analysis are visualised in graphical

Table 7. Rate of change shrub and grass vegetation area based on NDVI classification

NDVI classification	La Nina 2022 (ha)			El Nino 2023 (ha)		
	July	August	September	July	August	September
Water body	263	239	173	109	27	15
No vegetation	434	523	558	596	1613	2676
Low vegetation index	444	558	699	572	1221	1119
Moderate vegetation index	1047	1377	1721	1385	1182	516
High vegetation index	2272	1763	1310	1798	417	135

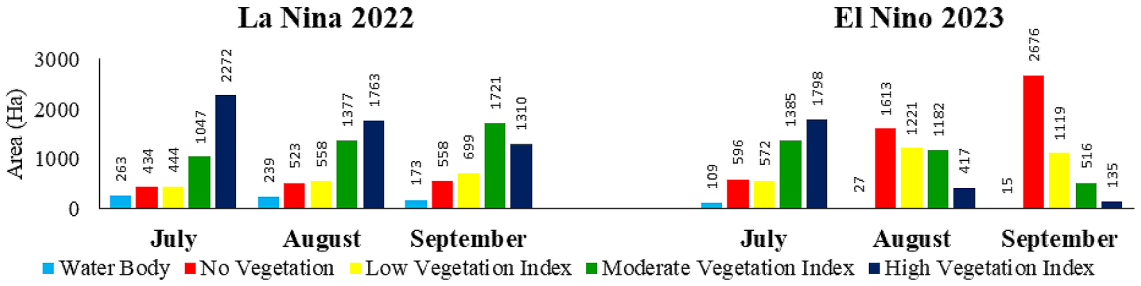

Figure 13 . Distribution of shrub and grass vegetation area based on NDVI

Table 8. Rate of change farmland vegetation area based on NDVI classification

NDVI classification	La Nina 2022 (ha)			El Nino 2023 (ha)		
	July	August	September	July	August	September
Water body	105	67	30	7	4	1
No vegetation	670	986	930	880	2437	3642
Low vegetation Index	755	973	1133	852	1114	662
Moderate vegetation Index	1381	1505	1649	1540	781	316
High vegetation Index	1834	1213	1002	1466	408	124

form in Figure 14 to facilitate interpretation of the changing trends.

Farmland vegetation dominated by rice and groundnuts also showed similar dynamics as the shrub and grass vegetation. During the La Nina phase in 2022, areas with medium to high vegetation indices were relatively stable, but during the El Nino phase in 2023, there was an increase in unvegetated areas and areas with low vegetation indices, especially in September. This can be attributed to the direct impact of drought, as agricultural land is highly vulnerable to extreme climate variability (Serkendiz et al., 2023). This condition inhibits plant growth, potentially reducing agricultural productivity in Gowa Regency. On the other hand, the presence of ENSO will make it difficult for farmers to predict the planting season because it can increase the uncertainty of seasonal transitions. In accordance with research conducted by Rahma & Ludwig, (2024), which conditions that farmers rely heavily on predictions of the dry and wet seasons, but ENSO has contributed to the uncertainty of the transition between the dry and wet seasons.

Relationship of climate parameters (rainfall and air temperature) to vegetation dynamics based on NDVI

Multicollinearity test

Multicollinearity test was conducted using the variance inflation factor (VIF) method to assess the relationship between rainfall and air temperature variables. The results of the analysis can be seen in Table 9.

The analysis results show that the VIF value for rainfall is 1.97, and for air temperature is also 1.97. These values are below the critical threshold (VIF < 5), which indicates that there is no significant multicollinearity problem between the two variables. Thus, both rainfall and air temperature can be used simultaneously in the regression model without causing bias in the parameter estimates. This result indicates that changes in one variable are not fully explained by the other, so they can be interpreted independently in further analyses.

Multiple linear regression analysis

The data used in this analysis consists of rainfall, air temperature, and vegetation area obtained from the results of NDVI analysis in July, August, and September during the La Nina phase in 2022 and the El Nino phase in 2023. The data presentation can be seen in Table 10.

In 2022, the average rainfall in July, August, and September was 59 mm, 63 mm, and 59 mm, respectively, with average air temperatures of 26.9 °C, 26.9 °C, and 27.2 °C. Meanwhile, in 2023, rainfall experienced significant changes, with values of 94 mm, 0 mm, and 0 mm respectively, while air temperature was recorded at 26.8 °C, 27.1 °C, and 28.3 °C. The vegetation area also fluctuates, ranging from 21,403 ha to 27,732 ha. The results of multiple linear regression analysis can be seen in Table 11.

The results of multiple linear regression analysis that shows the relationship between rainfall and air temperature on vegetation based on NDVI in the La Nina phase in 2022 and El Nino in 2023

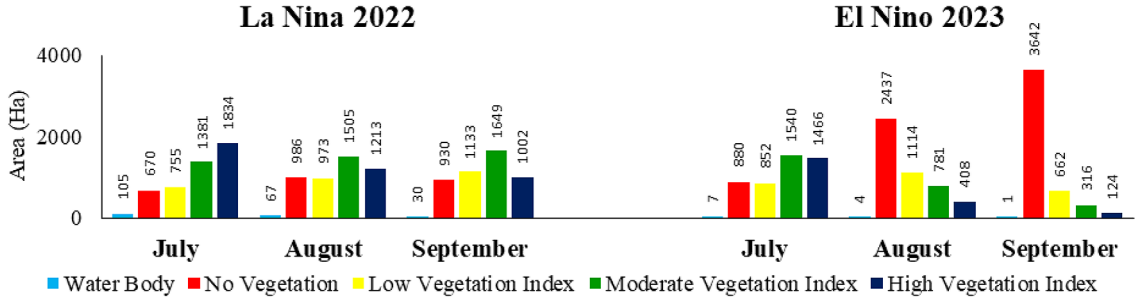

Figure 14. Distribution of farmland vegetation area based on NDVI

Table 9. Multicollinearity test results

Climate parameters	Variance inflation factor (VIF)	Test result
Rainfall	1.97	No multicollinearity
Air temperature	1.97	

Table 10. Rainfall, temperature, and vegetation data for multiple linear regression analysis

ENSO	Years	Month	Rainfall (mm)	Air temperature (°C)	Vegetation (ha)
La Nina phase	2022	July	59	26.9	27732
La Nina phase	2022	August	63	26.9	27330
La Nina phase	2022	September	59	27.2	27505
El Nino phase	2023	July	94	26.8	27585
El Nino phase	2023	August	0	27.1	24554
El Nino phase	2023	September	0	28.3	21403

Table 11. Multiple linear regression analysis results**.**

Variabel X	Coefficients (B)	Standar error	t-stat	p-value
Constant	97698.37	28794.17	3.39	0.043
Rainfall (X_1)	30.63	15.35	2.00	0.140
Air Temperature (X_2)	-2686.92	1040.20	-2.58	0.082

in Manuju and Parangloe Districts of Gowa Regency can be seen in the following equation:

$$\hat{Y} = 97698.37 + 30.63 \text{ Rainfall} - \\ - 2686.92 \text{ Air temperature} \quad (9)$$

The constant in the model has a value of 97,698.37 with a p-value of 0.043, indicating that the baseline vegetation value is statistically significant. However, interpretation of the constant needs to be done with caution, as in this case the zero value for the independent variable may not represent real conditions. The rainfall variable has a regression coefficient of 30.63 with a standard error of 15.35. The t-statistic value for this variable is 2.00 with a p value of 0.140. A p value greater than 0.05 indicates that rainfall does not have a significant effect on vegetation at the 95% confidence level. However, the positive coefficient indicates that an increase in rainfall has the potential to increase vegetation area, although it is not statistically significant. Furthermore, the air temperature variable has a regression coefficient of -2,686.92 with a standard error of 1,040.20. The t-statistic value for air temperature is -2.58 with a p value of 0.082. Although the p value is greater than 0.05, this result is close to the significance limit, indicating that air temperature may have a considerable influence on vegetation, but not at the 95% confidence level. The negative coefficient indicates that an increase in air temperature tends to decrease the area of vegetation.

Overall, the regression results show that the constants in the model are statistically significant, while the rainfall and air temperature variables have not shown significance at the 95% confidence level. However, air temperature has a potentially stronger influence than rainfall. The implications of these results suggest that air temperature factors may contribute more to variation in vegetation than rainfall, although additional modelling is required to increase statistical significance.

Based on Table 12, the regression model shows that 92% of vegetation variation can be explained by rainfall and air temperature (R^2 = 0.92), with an Adjusted R^2 = 0.87 value that remains stable after adjustment. The overall significance of the model (F = 17.63 and p-value = 0.02) indicates that rainfall and air temperature simultaneously have a significant influence on vegetation dynamics in the study area. In other words, the variability of the two climatic parameters jointly determines the dynamics of vegetation growth and distribution. However, as the independent variables were not individually significant at the 95% confidence level, additional analyses should be conducted to improve understanding of this relationship.

These findings reinforce the understanding that climate variability, based on precipitation and

Table 12. Regression model

Statistical model	Value
R^2	0.92
Adjusted R^2	0.87
F Statistics	17.63
p-value	0.02

air temperature, plays an important role in determining the structure and dynamics of vegetation ecosystems. Therefore, climate phenomena such as ENSO that affect rainfall and air temperature patterns can have a significant impact on ecosystem balance and vegetation survival in the long term. A holistic approach is needed for future research to comprehensively understand vegetation dynamics.

CONCLUSIONS

The results showed significant differences in vegetation dynamics between La Nina and El Nino phases. During the La Nina phase in 2022, NDVI showed stability and dominance of areas with high vegetation indices. Climatic variability in this phase is characterised by stable rainfall and air temperatures that support optimal vegetation growth. In contrast, during the El Nino phase in 2023, NDVI shows a significant decrease in areas with a high vegetation index and a significant increase in areas without vegetation. Climate variability during this phase is characterised by very low rainfall and higher air temperatures, which has implications for reduced productivity and vegetation degradation. In addition, regression analyses showed that air temperature tends to have a greater influence than rainfall on vegetation dynamics. The regression model has an $R^2 = 0.92$ and Adjusted $R^2 = 0.87$, indicating strong predictive ability. Partially, the two variables showed no significant influence at the 95% confidence level. However, based on F statistics ($F = 17.63$; $p = 0.02$), both variables simultaneously had a significant influence on vegetation. This research can be used as a basis for formulating mitigation and adaptation strategies to climate variability in the future.

Acknowledgments

The authors would like to thank all academicians of the Environmental Management Study Programme, Postgraduate School, and Hasanuddin University for their support and guidance in the preparation of this article. Thanks also go to the Meteorology, Climatology, and Geophysics Centre (BMKG) Region IV Makassar and the Food Crops and Horticulture Office of Gowa Regency for providing the facilities and data needed for this research.

REFERENCES

1. Adinda, R., Rusdi, M., & Sugianto, S. (2020). Pemanfaatan Indeks Vegetasi NDVI Terhadap Siklus Phenology Tanaman Padi Pada Musim Gadu 2017. *Jurnal Ilmiah Mahasiswa Pertanian*, *5*(2), 301–309. https://doi.org/10.17969/jimfp.v5i2.14873
2. Akbar, M. R., Arisanto, P. A. A., Sukirno, B. A., Merdeka, P. H., Priadhi, M. M., & Zallesa, S. (2020). Mangrove vegetation health index analysis by implementing NDVI (normalized difference vegetation index) classification method on sentinel-2 image data case study: Segara Anakan, Kabupaten Cilacap. *IOP Conference Series: Earth and Environmental Science*, *584*(1), 012069. https://doi.org/10.1088/1755-1315/584/1/012069
3. Akinwande, M. O., Dikko, H. G., & Samson, A. (2015). Variance Inflation Factor: As a Condition for the Inclusion of Suppressor Variable(s) in Regression Analysis. *Open Journal of Statistics*, *05*(07), 754–767. https://doi.org/10.4236/ojs.2015.57075
4. Amanollahi, J., Abdullah, A. M., Ramli, M. F., & Pirasteh, S. (2012). Land Surface Temperature Assessment in Semi-Arid Residential Area of Tehran, Iran Using Landsat Imagery. *World Applied Sciences Journal 20*, *2*, 319–326. https://doi.org/10.5829/idosi.wasj.2012.20.02.3661
5. Aquino, D. D. N., Rocha Neto, O. C. D., Moreira, M. A., Teixeira, A. D. S., & Andrade, E. M. D. (2018). Use of remote sensing to identify areas at risk of degradation in the semi-arid region. *REVISTA CIÊNCIA AGRONÔMICA*, *49*(3). https://doi.org/10.5935/1806-6690.20180047
6. Arjasakusuma, S., Yamaguchi, Y., Hirano, Y., & Zhou, X. (2018). ENSO- and Rainfall-Sensitive Vegetation Regions in Indonesia as Identified from Multi-Sensor Remote Sensing Data. *ISPRS International Journal of Geo-Information*, *7*(3), 103. https://doi.org/10.3390/ijgi7030103
7. Atun, R., Kalkan, K., & Gürsoy, Ö. (2020). Determining The Forest Fire Risk with Sentinel 2 Images. *Turkish Journal of Geosciences*, *1*(1), 22–26.
8. Aziz, A., Umar, M., Mansha, M., Khan, M. S., Javed, M. N., Gao, H., Farhan, S. B., Iqbal, I., & Abdullah, S. (2018). Assessment of drought conditions using HJ-1A/1B data: A case study of Potohar region, Pakistan. *Geomatics, Natural Hazards and Risk*, *9*(1), 1019–1036. https://doi.org/10.1080/19475705.2018.1499558
9. Bao, Z., Zhang, J., Wang, G., Guan, T., Jin, J., Liu, Y., Li, M., & Ma, T. (2021). The sensitivity of vegetation cover to climate change in multiple climatic zones using machine learning algorithms. *Ecological Indicators*, *124*, 107443. https://doi.org/10.1016/j.ecolind.2021.107443
10. Bid, S. (2016). Change Detection of Vegetation

Cover by NDVI Technique on Catchment Area of the Panchet Hill Dam, India. *International Journal of Research in Geography*, *2*(3), 11–20. https://doi.org/10.20431/2454-8685.0203002

11. BMKG. (2022). *INDONESIA - Pemantauan Dampak Bencana Hidrometeorologis Juli – September (Q3) 2022*. Badan Meteorologi, Klimatologi, dan Geofisika (BMKG). https://www.bmkg.go.id/iklim/buletin-iklim/pemantauan-dampak-bencana-hidrometeorologis-juli-september-q3-2022
12. BMKG. (2023). *Buletin Pemantauan Musiman Indonesia Juli – September (Q3) 2023*. Badan Meteorologi, Klimatologi, dan Geofisika (BMKG). https://www.bmkg.go.id/iklim/buletin-iklim/pemantauan-musiman-april-september-q3-2023
13. Chueasa, B., Humphries, U. W., & Waqas, M. (2024). Influence of El Niño southern oscillation on precipitation variability in Northeast Thailand. *MethodsX*, *13*, 102954. https://doi.org/10.1016/j.mex.2024.102954
14. Damette, O., Mathonnat, C., & Thavard, J. (2024). Climate and sovereign risk: The Latin American experience with strong ENSO events. *World Development*, *178*, 106590. https://doi.org/10.1016/j.worlddev.2024.106590
15. Didion-Gency, M., Gessler, A., Buchmann, N., Gisler, J., Schaub, M., & Grossiord, C. (2022). Impact of warmer and drier conditions on tree photosynthetic properties and the role of species interactions. *New Phytologist*, *236*(2), 547–560. https://doi.org/10.1111/nph.18384
16. Galar, M., Sesma, R., Ayala, C., & Aranda, C. (2019). Super-Resolution For SENTINEL-2 Images. *The International Archives of the Photogrammetry, Remote Sensing and Spatial Information Sciences*, *XLII-2/W16*, 95–102. https://doi.org/10.5194/isprs-archives-XLII-2-W16-95-2019
17. Kemarau, R. A., & Eboy, O. V. (2021). The Impact of El Niño–Southern Oscillation (ENSO) on Temperature: A Case Study in Kuching, Sarawak. *Malaysian Journal of Social Sciences and Humanities (MJSSH)*, *6*(1), 289–297. https://doi.org/10.47405/mjssh.v6i1.602
18. Kurniadi, A., Weller, E., Min, S., & Seong, M. (2021). Independent ENSO and IOD impacts on rainfall extremes over Indonesia. *International Journal of Climatology*, *41*(6), 3640–3656. https://doi.org/10.1002/joc.7040
19. Le, T. (2023). Increased impact of the El Niño–Southern Oscillation on global vegetation under future warming environment. *Scientific Reports*, *13*(1), 14459. https://doi.org/10.1038/s41598-023-41590-8
20. Letts, M. G., Johnson, D. R. E., & Coburn, C. A. (2010). Drought stress ecophysiology of shrub and grass functional groups on opposing slope aspects of a temperate grassland valley. *Botany*, *88*(9), 850–866. https://doi.org/10.1139/B10-054
21. Li, H., Hu, Y., & Batunacun. (2024). Responses of vegetation low-growth to extreme climate events on the Mongolian Plateau. *Global Ecology and Conservation*, *56*, e03292. https://doi.org/10.1016/j.gecco.2024.e03292
22. Li, X., Xu, J., Jia, Y., Liu, S., Jiang, Y., Yuan, Z., Du, H., Han, R., & Ye, Y. (2024). Spatio-temporal dynamics of vegetation over cloudy areas in Southwest China retrieved from four NDVI products. *Ecological Informatics*, *81*, 102630. https://doi.org/10.1016/j.ecoinf.2024.102630
23. Martinez, A. D. L. I., & Labib, S. M. (2023). Demystifying normalized difference vegetation index (NDVI) for greenness exposure assessments and policy interventions in urban greening. *Environmental Research*, *220*, 115155. https://doi.org/10.1016/j.envres.2022.115155
24. Mazzarella, A., Giuliacci, A., & Liritzis, I. (2010). On the 60-month cycle of multivariate ENSO index. *Theoretical and Applied Climatology*, *100*(1–2), 23–27. https://doi.org/10.1007/s00704-009-0159-0
25. Mehmood, K., Anees, S. A., Rehman, A., Pan, S., Tariq, A., Zubair, M., Liu, Q., Rabbi, F., Khan, K. A., & Luo, M. (2024). Exploring spatiotemporal dynamics of NDVI and climate-driven responses in ecosystems: Insights for sustainable management and climate resilience. *Ecological Informatics*, *80*, 102532. https://doi.org/10.1016/j.ecoinf.2024.102532
26. Mishra, V., Tiwari, A. D., & Kumar, R. (2022). Warming climate and ENSO variability enhance the risk of sequential extremes in India. *One Earth*, *5*(11), 1250–1259. https://doi.org/10.1016/j.oneear.2022.10.013
27. Nugroho, C. A., & Setiawan, A. W. (2022). Pengaruh Frekuensi Penyiraman Dan Volume Air Terhadap Pertumbuhan Sawi Pakcoy Pada Media Tanam Campuran Arang Sekam Dan Pupuk Kandang. *Agrium*, *25*(1), 12–23. https://doi.org/10.30596/agrium.v25i1.8471
28. Nur'utami, M. N., & Hidayat, R. (2016). Influences of IOD and ENSO to Indonesian Rainfall Variability: Role of Atmosphere-ocean Interaction in the Indo-pacific Sector. *Procedia Environmental Sciences*, *33*, 196–203. https://doi.org/10.1016/j.proenv.2016.03.070
29. Rahma, A. D., & Ludwig, F. (2024). El Nino Effects on Water Availability for Agriculture: Case Study of Magelang, Central Java, Indonesia. *Applied Environmental Research*, *4*(2), 19. https://doi.org/10.35762/AER.2024019
30. Šandera, J., & Štych, P. (2020). Selecting Relevant Biological Variables Derived from Sentinel-2 Data for Mapping Changes from Grassland to Arable

Land Using Random Forest Classifier. *Land*, *9*(11), 420. https://doi.org/10.3390/land9110420

31. Santoso, A., Mcphaden, M. J., & Cai, W. (2017). The Defining Characteristics of ENSO Extremes and the Strong 2015/2016 El Niño. *Reviews of Geophysics*, *55*(4), 1079–1129. https://doi.org/10.1002/2017RG000560
32. Sarvina, Y. (2023). Enso and climate variability in Papua. *IOP Conference Series: Earth and Environmental Science*, *1192*(1), 012041. https://doi.org/10.1088/1755-1315/1192/1/012041
33. Serkendiz, H., Tatli, H., Özcan, H., Çetin, M., & Sungur, A. (2023). Multidimensional assessment of agricultural drought vulnerability based on socio-economic and biophysical indicators. *International Journal of Disaster Risk Reduction*, *98*, 104121. https://doi.org/10.1016/j.ijdrr.2023.104121
34. Shrestha, N. (2020). Detecting Multicollinearity in Regression Analysis. *American Journal of Applied Mathematics and Statistics*, *8*(2), 39–42. https://doi.org/10.12691/ajams-8-2-1
35. Stuecker, M. F. (2023). The climate variability trio: Stochastic fluctuations, El Niño, and the seasonal cycle. *Geoscience Letters*, *10*(1), 51. https://doi.org/10.1186/s40562-023-00305-7
36. Sun, G.-Q., Li, L., Li, J., Liu, C., Wu, Y.-P., Gao, S., Wang, Z., & Feng, G.-L. (2022). Impacts of climate change on vegetation pattern: Mathematical modeling and data analysis. *Physics of Life Reviews*, *43*, 239–270. https://doi.org/10.1016/j.plrev.2022.09.005
37. Sureiman, O., & Mangera, C. (2020). F-test of overall significance in regression analysis simplified. *Journal of the Practice of Cardiovascular Sciences*, *6*(2), 116. https://doi.org/10.4103/jpcs.jpcs_18_20
38. Uyanık, G. K., & Güler, N. (2013). A Study on Multiple Linear Regression Analysis. *Procedia - Social and Behavioral Sciences*, *106*, 234–240. https://doi.org/10.1016/j.sbspro.2013.12.027
39. Wang, G., Cai, W., & Santoso, A. (2020). Stronger Increase in the Frequency of Extreme Convective than Extreme Warm El Niño Events under Greenhouse Warming. *Journal of Climate*, *33*(2), 675–690. https://doi.org/10.1175/JCLI-D-19-0376.1
40. Wiel, K. V. D., & Bintanja, R. (2021). Contribution of climatic changes in mean and variability to monthly temperature and precipitation extremes. *Communications Earth & Environment*, *2*(1), 1. https://doi.org/10.1038/s43247-020-00077-4
41. Winkler, D. E., Belnap, J., Hoover, D., Reed, S. C., & Duniway, M. C. (2019). Shrub persistence and increased grass mortality in response to drought in dryland systems. *Global Change Biology*, *25*(9), 3121–3135. https://doi.org/10.1111/gcb.14667
42. Xu, N., Cai, D., & Zhao, X. (2024). Constructing a eucalyptus identification model based on NDVI time-series remote sensing images. *CATENA*, *238*, 107846. https://doi.org/10.1016/j.catena.2024.107846
43. Zhihao, W., & Fang, W. (2024). UV-NDVI for real-time crop health monitoring in vertical farms. *Smart Agricultural Technology*, *8*, 100462. https://doi.org/10.1016/j.atech.2024.100462
44. Zhu, A., Xu, H., Deng, J., Ma, J., & Li, S. (2021). El Niño–Southern Oscillation (ENSO) effect on interannual variability in spring aerosols over East Asia. *Atmospheric Chemistry and Physics*, *21*(8), 5919–5933. https://doi.org/10.5194/acp-21-5919-2021